Endoscopic optical coherence tomography with a modified microelectromechanical systems mirror for detection of bladder cancers

Tuqiang Xie, Huikai Xie, Gary K. Fedder, and Yingtian Pan

Experimental results of a modified micromachined microelectromechanical systems (MEMS) mirror for substantial enhancement of the transverse laser scanning performance of endoscopic optical coherence tomography (EOCT) are presented. Image distortion due to buckling of MEMS mirror in our previous designs was analyzed and found to be attributed to excessive internal stress of the transverse bimorph meshes. The modified MEMS mirror completely eliminates bimorph stress and the resultant buckling effect, which increases the wobbling-free angular optical actuation to greater than 37°, exceeding the transverse laser scanning requirements for EOCT and confocal endoscopy. The new optical coherence tomography (OCT) endoscope allows for two-dimensional cross-sectional imaging that covers an area of 4.2 mm × 2.8 mm (limited by scope size) and at roughly 5 frames/s instead of the previous area size of 2.9 mm × 2.8 mm and is highly suitable for noninvasive and high-resolution imaging diagnosis of epithelial lesions *in vivo*. EOCT images of normal rat bladders and rat bladder cancers are compared with the same cross sections acquired with conventional bench-top OCT. The results clearly demonstrate the potential of EOCT for *in vivo* imaging diagnosis and precise guidance for excisional biopsy of early bladder cancers.

OCIS codes: 170.2150, 170.3880, 170.4500, 170.7230, 170.3890.

1. Introduction

Optical coherence tomography (OCT) is a new optical imaging technique that can provide cross-sectional images of biological tissue, highly desirable for imaging diagnosis of superficial lesions and the prognosis of these lesions.[1] OCT technology has been widely applied to image various biological tissue such as eye, skin, tooth, gastrointestinal tracts, respiratory tracts, genitourinary tracts, and urinary bladder.[2,3] It can delineate tissue micromorphology, holding the potential for noninvasive optical biopsy or optically guided biopsy. In contrast to excisional biopsy that presents hazards to patients or that may accelerate or undesirably alter a pathologic process, OCT is a safer and instantaneous *in situ* decision tool during the course of surgery. In recent years, the development of real-time, high-performance, reliable and low-cost OCT catheters and endoscopes has been drawing more attention for future clinical applications.[2–5] Various attempts of transverse laser scanning techniques have been employed to miniaturize lateral scanning probes to fit into slender endoscopes, including a rotary fiber-optic joint connected to a 90° deflecting microprism or a small galvanometric plate swinging the distal fiber tip.[2,3] However, the rotary fiber joint is more suitable to image the circumference of intraluminal tracts and the galvo or piezoelectric transducer swinger has a limited range (<2 mm) for transverse scanning.[2]

Recently, microelectromechanical systems (MEMS) have obtained extensive attention and found enormous applications in biomedical areas because of their small sizes, low consuming energy, nominal forces, and flexibility. For instance, large and flat MEMS mirrors with a large tunable actuation angle are highly desirable for applications such as laser scanning and medical imaging. A recent report of EOCT utilizing a MEMS mirror for endoscopic laser scanning has been proposed by the authors, showing a great promise.[4,5] However, buckling of the em-

T. Xie and Y. Pan (yingtian.pan@sunysb.edu) are with the Department of Biomedicine Engineering, State University of New York at Stony Brook HSC 918, Room 030, Stony Brook, New York 11794-8181. H. Xie is with the Department of Electrical and Computer Engineering, University of Florida, Gainesville, Florida 32611. G. K. Fedder is with the Department of Electrical and Computer Engineering, Carnegie Mellon University, 5000 Forbes Avenue, Pittsburgh, Pennsylvania 15213.

Received 24 June 2003.
0003-6935/03/316422-05$15.00/0

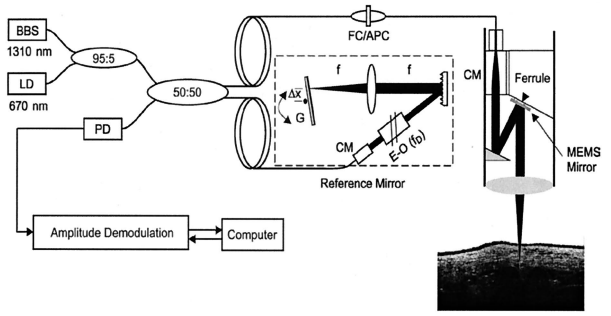

Fig. 1. Schematic of EOCT with a MEMS mirror. BBS, broadband light source; LD, aiming laser; PD, photodiode; CM, fiber-optic collimator.

ployed bimorph mesh structure causes an ~10° discontinuity in the angular actuation curve, severely limiting the usable range of the transverse laser scanning. In this paper, we present an improved OCT endoscope using a modified single-crystalline Si micromirror that completely eliminates buckling and allows transverse scanning over 37°. This EOCT catheter allows for two-dimensional (2D) cross-sectional imaging that covers an area of 4.2 mm × 2.8 mm (limited by scope size) instead of the previous area size of 2.9 mm × 2.8 mm. Preliminary results based on animal studies are presented, including comparisons with bench-top OCT to demonstrate the technological improvement.

2. Methods and Materials

Figure 1 depicts the schematic of the new endoscopic OCT system, which is based on a fiber-optic Michelson interferometer. The broadband light source used for illumination has a pigtailed output power of 13 mW, a central wavelength of 1320 nm, and a spectral bandwidth of 77 nm, yielding a coherence length of 10 μm. In the reference arm of the optical fiber interferometer, the light from the fiber endface is coupled into a ϕ2 mm collimated beam by an angle-polished gradient-index lens. The collimated light beam is then guided to a high-speed depth scanning unit that contains a rapid grating-lens-based optical delay line, as has been previously reported.[6,7] The light in the sample arm is collimated by a custom fiber-optic aspherical lens to a beam size of 0.75 mm, deflected by a conventional mirror and a transversely scanning MEMS mirror. It is then focused by an $f =$ 10 mm scan lens onto the surface of the biological tissue under examination, and the backscattered light exiting the specimen is collected by the same optics. The OCT scope, which includes the connection fiber, the transverse scanning optics, is integrated into the instrument channel of a standard endoscope.

The MEMS mirror employed in the EOCT catheter for transverse laser scanning is critical to image fidelity of the EOCT system. The enhancement of laser scanning performance and its influence on OCT image fidelity have been evaluated with assembled and tested EOCT scopes that employ both generations of the MEMS mirrors. Both MEMS mirrors employ a bimorph actuator with an integrated polysilicon heater to actuate an Al-coated mirror with active area of 1 mm × 1 mm. The primary difference of the two MEMS mirrors is the bimorph structure, which is crucial to the performance of MEMS angular actuation. A scanning electron micrograph (SEM) of the first-generation mirror is shown in Fig. 2, in which the bimorph actuator is a mesh of cross-connected beams. The beams are composed of a 0.7-μm-thick Al layer coated on top of a 1.2-μm-thick SiO_2 layer embedded with a 0.2-μm-thick poly-Si layer. The mirror is coated with a 0.7-μm-thick Al layer, and the underlying 40-μm-thick single-crystal Si makes the mirror flat. The mesh curls up after release as a result of tensile stress in the Al layer and compressive residual stress in the bottom SiO_2 layers. Figure 3 shows the test result of the first-

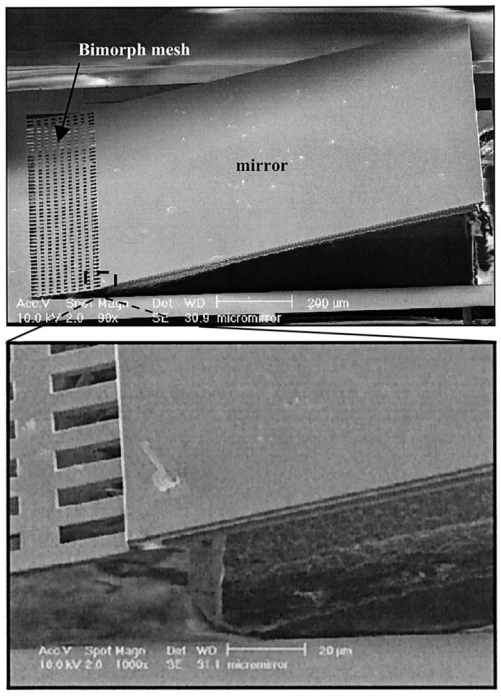

Fig. 2. SEM of an old MEMS mirror.

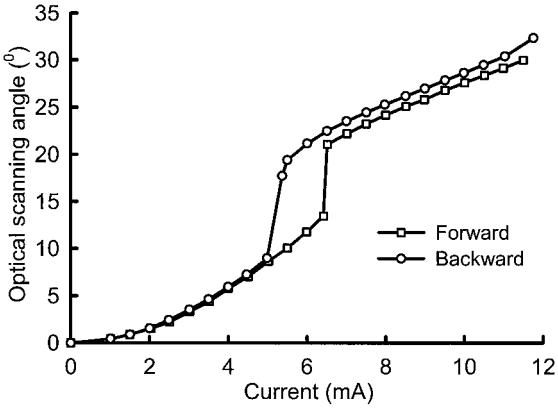

Fig. 3. Characteristic curve of MEMS mirror.

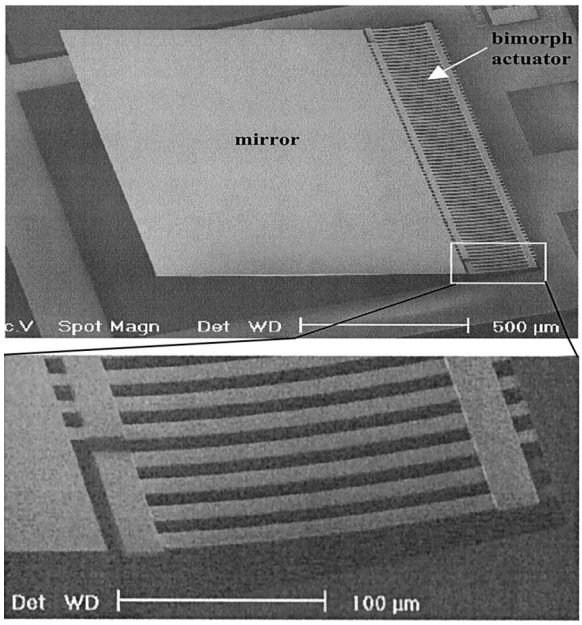

Fig. 4. SEM of the modified MEMS mirror.

generation mirror. Although the angular actuation range can be up to 35°, wobbling and hysterysis are noticeable. As wobbling occurs in the intermediate range, the usable range of the first-generation MEMS mirror is severely limited. In our previous EOCT, wobbling was avoided by a large (9°) preset angle on the ferrule. Nevertheless, the usable scanning angle was decreased to ~13°, limiting the wobbling-free transverse scanning range to 2.9 mm or less.

Further studies have revealed that hysterysis is caused by thermal relaxation, and wobbling occurred because of buckling of the mesh beams as a result of excessive thermal stress and expansion in the transverse direction. To eliminate this adverse effect, short transverse beams in the bimorph mesh are removed, and thus the bimorph mesh becomes a set of parallel beams as shown in Fig. 4. Since the bimorph beams can move freely along the longitudinal direction, buckling in both transverse and longitudinal directions is eliminated. Figure 5 shows the test result of the second-generation MEMS mirror with

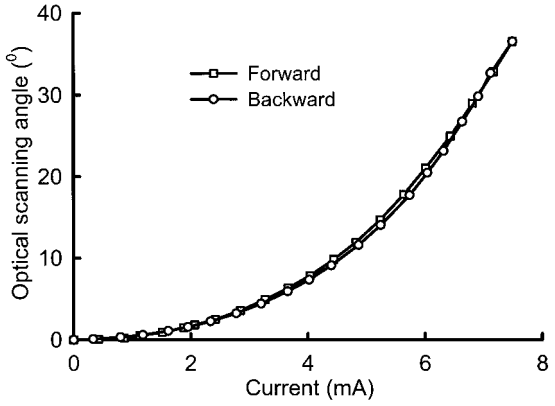

Fig. 5. Characteristic curve of MEMS mirror.

angular actuation of roughly 37°. This permits a wobbling-free transverse laser scan over 6.6 mm, exceeding the full range of the endoscope tube, which is only 4.3 mm. In particular, because the curve is monotonic and smooth with less than ±2% hysteretic error, linear actuation can be easily implemented by a simple nonlinear correction to allow artifact-free full-range EOCT imaging.

To examine EOCT technology in identifying various morphologic changes associated with epithelial tumors, we imaged tumorigenesis in rat bladders by both EOCT and bench-top OCT. In this study, based on a well-developed bladder cancer model, Fisher rats were exposed to methyl-nitroso-urea to develop transitional cell carcinomas in the bladders. Acute responses of methyl-nitroso-urea treatment included disruption to the urothelium and inflammatory lesions followed by chronic diseases, including dysplasia and frank transitional cancers. The excised bladder for imaging diagnosis was pinned onto a ring holder placed in a modified Ringer's buffer solution at 37 °C, which maintained the physiologic functions of the rat bladder, preserving muscle contractility and epithelial permeability according to previous studies. When OCT imaging was performed with both the bench-top and the endoscopic setups, a visible light beam was used as guidance to image proximately the same lateral positions on the tissues. Here *ex vivo* study was performed because there is lack of cancer model for large animals such as pigs to allow for *in vivo* examinations.

3. Results

To examine the influence of the MEMS mirrors on EOCT image fidelity, we performed a comparative image study on normal rabbit bladders *ex vivo*. The results are shown in Fig. 6. Morphologic details of rabbit bladder, e.g., urothelium (U), lamina propria (LP) or submucosa, and muscular layer (M) can be delineated in both images. However, artifacts due to MEMS mirror wobbling are noticeable in panel (A), limiting the usable lateral imaging range to be less than 2.6 mm for the EOCT catheter with the old MEMS mirror. On the contrary, the image acquired with the EOCT with the modified MEMS mirror (panel B) is wobble free over the full range of the EOCT sheath (4.3 mm). The result of this comparative study clearly demonstrates the capability of the modified MEMS mirror for high-fidelity full-range endoscopic OCT imaging.

According to our previous studies, the bench-top OCT is capable of delineating micromorphologic details of the bladder, e.g., urothelium, lamina propria, and muscular layer, based on backscattering difference in these layers, and of tracking characteristic changes due to tumorigenesis, including hyperplasia and neoplasia.[8,9] Figure 6 demonstrates that EOCT can identify micromorphology of bladder, thus holding a great promise for endoscopic *in vivo* imaging diagnosis of early bladder cancers. To further examine the utility of EOCT for epithelial cancer imaging, we performed a comparative study on rat bladder

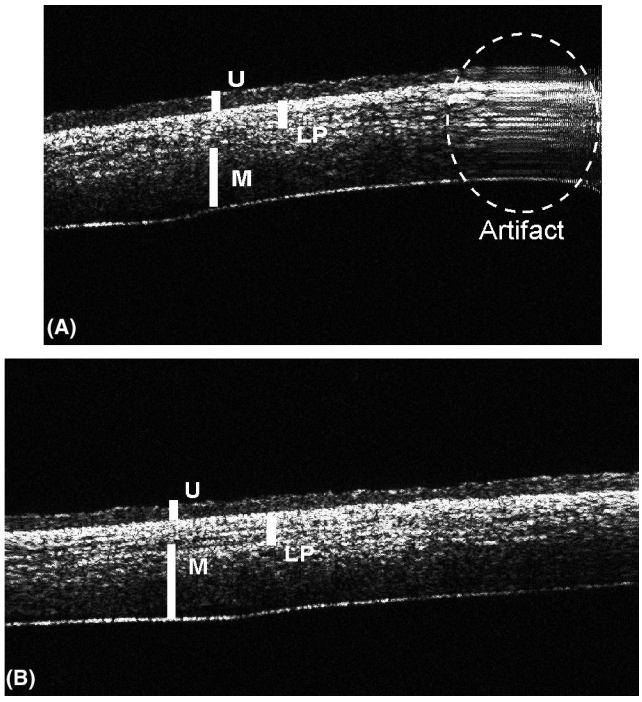

Fig. 6. Rabbit bladder imaged *ex vivo* by EOCT (A) with old MEMS mirror and (B) modified MEMS mirror. Image size: 3.6 mm × 2 mm (A) and 4.3 mm × 2 mm (B). U, urothelium; LP, lamina propria; M, muscular layer. Artifact due to mirror wobbling is noticeable in (A).

cancers, in which the same cross section on a rat bladder cancer was imaged with the EOCT probe (B) and the benchtop OCT (A). The results are presented in Figs. 7 and 8. Since it was very difficult to ensure that the bench-top OCT probe and the EOCT

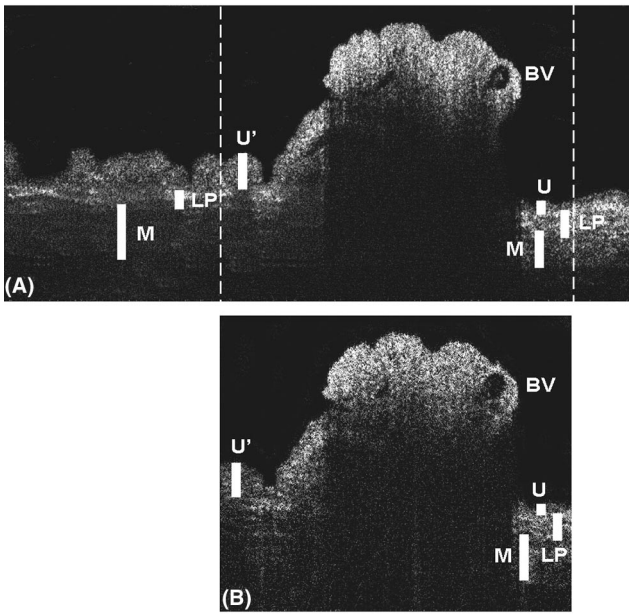

Fig. 7. Rat bladder cancer with larger papillary hyperplasia imaged with (A) bench-top OCT and (B) EOCT. Image size: (A) 6 mm × 2 mm and (B) 3.3 mm × 2 mm.

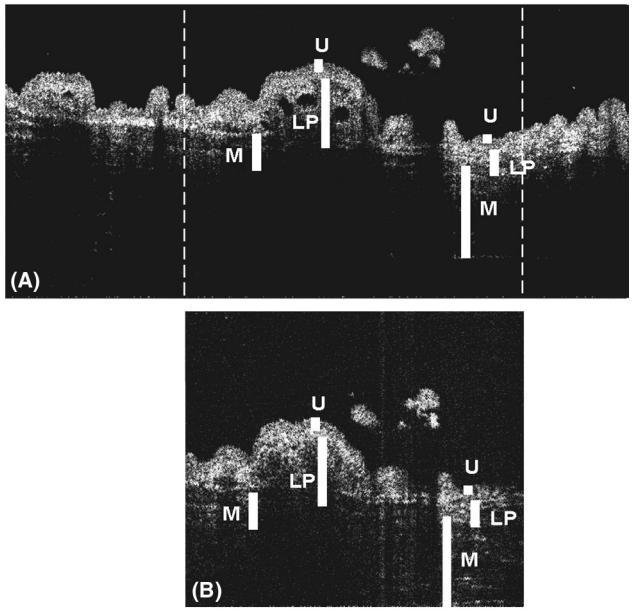

Fig. 8. Rat bladder cancer with early papillary hyperplasia imaged with (A) bench-top OCT and (B) EOCT. Image size: (A) 6 mm × 2 mm and (B) 3.3 mm × 2 mm.

catheter scanned across the exact same positions, there is slight difference between the two OCT images in Fig. 8. Despite slightly degraded image fidelity (e.g., slightly decreased signal-to-noise ratio and lateral resolution), detailed morphologic changes of the bladder cancer imaged in two OCT systems are closely comparable. These include identification of normal and hyperplastic urothelia (U, U′), lamina propria (LP) or submucosa, and muscular layer (M). More important, backscattering increase in the thick neoplastic urothelium, including heavy vascularization (BV) is clearly shown in the EOCT image. These results justify the application of EOCT for *in vivo* human study for diagnosis and more precise staging of early bladder cancers.

4. Conclusion

In summary, we have presented MEMS-based EOCT for bladder cancer imaging. The modified MEMS mirror allows wobbling-free, full-range (4.3 mm), two-dimensional OCT imaging at ~5 frames/s.[10] Results of animal studies show that the new EOCT can clearly delineate morphologic details of bladder and detect cancerous changes, thus demonstrating the potential of this technology for *in vivo* clinical uses. The axial resolution of EOCT is roughly 10 μm; whereas the lateral resolution is close to 20 μm (limited with a ϕ0.75 mm fiber collimator), resulting in degraded image contrast and increased speckle noise. Further improvement includes utilizing a custom large beam size (e.g., ϕ1 mm) collimator to improve the transverse resolution. The resonant frequency of the modified MEMS mirror is 165 Hz, well exceeding the speed requirement for most endoscopic laser scanning applications. More important, the superior performance of the modified MEMS mir-

ror (e.g., large scanning range and good linearity) suggests its applications in other laser scanning imaging techniques such as confocal and multiphoton excitation endoscopy.

This research is supported in part by National Institutes of Health contract R01-DK059265 (Y.P.), the Whitaker Foundation contract 00-0149 (Y.P.), and by Defense Advance Research Projects Agency contract F30602-97-2-0323 (G.K.F.).

References

1. J. G. Fujimoto, "Optical coherence tomography: a new view toward biomedical imaging," Photonics Spectra **32,** 114–115 (1998).
2. A. M. Sergeev, V. M. Gelikonov, G. V. Gelikonov, F. I. Feldchtein, R. V. Kuranov, N. D. Gladkova, N. M. Shakhova, L. B. Snopova, A. V. Shakhov, I. A. Kuznetzova, A. N. Denisenko, V. V. Pochinko, Y. P. Chumakov, and O. S. Streltzova, "*In vivo* endoscopic OCT imaging of precancer and cancer states of human mucosa," Opt. Express **1,** 432–440 (1997); http://www.opticsexpress.org.
3. G. J. Tearney, M. E. Brezinski, B. E. Bouma, S. A. Boppart, C. Pitris, J. F. Southern, and J. G. Fujimoto, "*In vivo* endoscopic optical biopsy with optical coherence tomography," Science **276,** 2037–2039 (1997).
4. Y. Pan, H. Xie, and G. K. Fedder, "Endoscopic optical coherence tomography based on a microelectromechanical mirror," Opt. Lett. **26,** 1966–1968 (2001).
5. T. Xie, H. Xie, G. K. Fedder, M. Zeidel, and Y. Pan, "Endoscopic optical coherence tomography with a micromachined mirror," in *Second Annual International IEEE-Engineering in Medicine and Biology Society Special Topic Conference on Microtechnologies in Medicine and Biology*, A. Dittmar and D. Beebe, eds. (IEEE, Piscataway, N.J., 2002), pp. 208–211.
6. A. M. Rollins, R. Ung-arunyawee, A. Chak, C. K. Wong, K. Kobayashi, M. V. Sivak, Jr., and J. A. Izatt, "Real-time *in vivo* image of human gastrointestinal ultrastructure by use of endoscopic optical coherence tomography with a novel efficient interferometer design," Opt. Lett. **24,** 1358–1360 (1999).
7. T.-Q. Xie, M. L. Zeidel, and Y.-T. Pan, "Detection of tumorigenesis in urinary bladder with optical coherence tomography: optical characterization of morphological changes," Opt. Express **10,** 1431–1443 (2002), http://www.opticsexpress.org.
8. T. Xie, Z. Li, M. L. Zeidel, and Y. Pan, "Optical imaging diagnostics of bladder tissue with optical coherence tomography," in *Lasers in Surgery: Advanced Characterization, Therapeutics, and Systems XII*, K. E. Bartels, L. S. Bass, W. T. de Riese, K. W. Gregory, A. Katzir, N. Kollias, M. D. Lucroy, R. S. Malek, G. M. Peavy, H.-D. Reidenbach, D. S. Robinson, U. K. Shah, L. P. Tate, E. A. Trowers, B. J. Wong, and T. A. Woodward, eds. Proc. SPIE **4609,** 159–164 (2002).
9. Y.-T. Pan, J. P. Lavelle, S. Bastaky, S. Meyers, D. L. Farkas, and M. Zeidel, "Detection of tumorigenesis in rat bladders with optical coherence tomography," Med. Phys. **28,** 2432–2440 (2001).
10. T. Q. Xie, H. K. Xie, G. K. Fedder, and Y. T. Pan, "Endoscopic optical coherence tomography with a new MEMS mirror," Electron. Lett. (2003) (to be published).